ACS OMEGA

http://pubs.acs.org/journal/acsodf

Article

Research on the Genetic Mechanism of High-Temperature Groundwater in the Geothermal Anomalous Area of Gold Deposit—Application to the Copper Mine Area of Yinan Gold Mine

Huiyong Yin, Chengwei Zhang, Xinlong Zhou,* Tao Chen, Fangying Dong, Wenju Cheng, Ruqian Tang, Guoliang Xu, and Peng Jiao

Cite This: *ACS Omega* 2022, 7, 43231−43241

Read Online

ACCESS | Metrics & More | Article Recommendations

ABSTRACT: Geothermal energy is new, environmentally friendly, and clean energy, which is of great significance to realize energy saving and emission reduction. The study of the genesis mechanism of geothermal water is the key to its rational development and utilization. In this study, based on 14 sets of water samples from the eastern section of the copper well mining area of Yinan Gold Mine, mineral saturation index, isotope analysis ($\delta^{18}O$, δD), Si-enthalpy mixing equation, and geochemical geothermal temperature scale were used to analyze the thermal storage temperature, recharge characteristics, mixing ratio, circulation depth, and fluid passage to reveal the geothermal water fugitive transmission pattern and genesis mechanism in the study area and to propose a geothermal water genesis model. The study shows that the water supply elevation in the area is between 687.22 and 1164.15 m and a large amount of cold water recharged it. It is inferred that the recharge area is the precipitation in the Northwest Mountain range and surrounding atmosphere. Groundwater flows along the fracture zone in a south-easterly direction. It receives heating from the surrounding rocks, where the water level rises at the fracture zone intersection and is stored in the lower and middle Cambrian thermal reservoirs and continues to receive heating from deeper heat sources. Based on this study and previous regional research data, the fault structure in this area is within the influence range of the energy field of the Yishu fault zone. Yishu fault zone becomes the heating source under the background of cold water. It is inferred that the east−east Yishu fault zone in the study area may also be the recharge area.

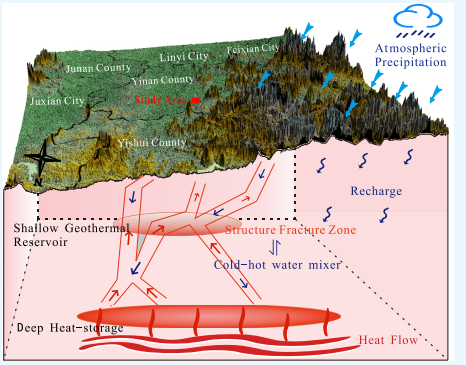

1. INTRODUCTION

The progress of society is inevitably accompanied by the increasing supply of various types of energy. Among the many renewable and clean energy sources, geothermal resources have massive reserves, a wide range of uses, a massive latent economic value, a relatively simple development methodology, and a high energy utilization rate, so the development and utilization of geothermal energy have received widespread attention.[1−3] According to surface outcrops and prospecting engineering exposures, the underground water temperature in the copper well mining area of Yinan Gold Mine can reach a maximum of 73.19 °C, presenting a geothermal anomaly, which has a certain impact on the efficient mining and production of the mine, so it is important and necessary to study the mechanism of the genesis of geothermal water in the geothermal anomaly area of the study area.

The key to geothermal water resources and efficient utilization lies in studying the hydrogeological conditions and formation mechanisms of geothermal anomalies.[4] White[5] first proposed the classical model for the formation of geothermal systems, namely, the infiltration of atmospheric precipitation and the timely emergence of hot springs under constant heating, summarizing the genesis model for low- and medium-temperature geothermal systems. Chiocchini[6] reconstructs the stratigraphic and tectonic setting of the Chimini Mountains and the Viterbo region of Italy, identifying the sources of hot water in both areas. A multidisciplinary approach, including stratigraphy, tectonics, geophysics, geochemistry, hydrogeology, and physical characteristics of the aquifers, was used to model this, which is rare in hydrogeological studies. Battistel[7] determined the recharge area of the geothermal water in the Cimino-Vico volcanic district by chemical and δD, $\delta^{18}O$, $^{87}Sr/^{86}Sr$, and $\delta^{11}B$ isotopic analyses to identify recharge areas and fluid pathways for geothermal water.

The predecessors analyzed and studied the geothermal resources around the Yishu fault zone. Yang[8] used shallow

Received: September 13, 2022
Accepted: November 1, 2022
Published: November 16, 2022

ACS Publications

© 2022 The Authors. Published by American Chemical Society

https://doi.org/10.1021/acsomega.2c05936
ACS Omega 2022, 7, 43231−43241

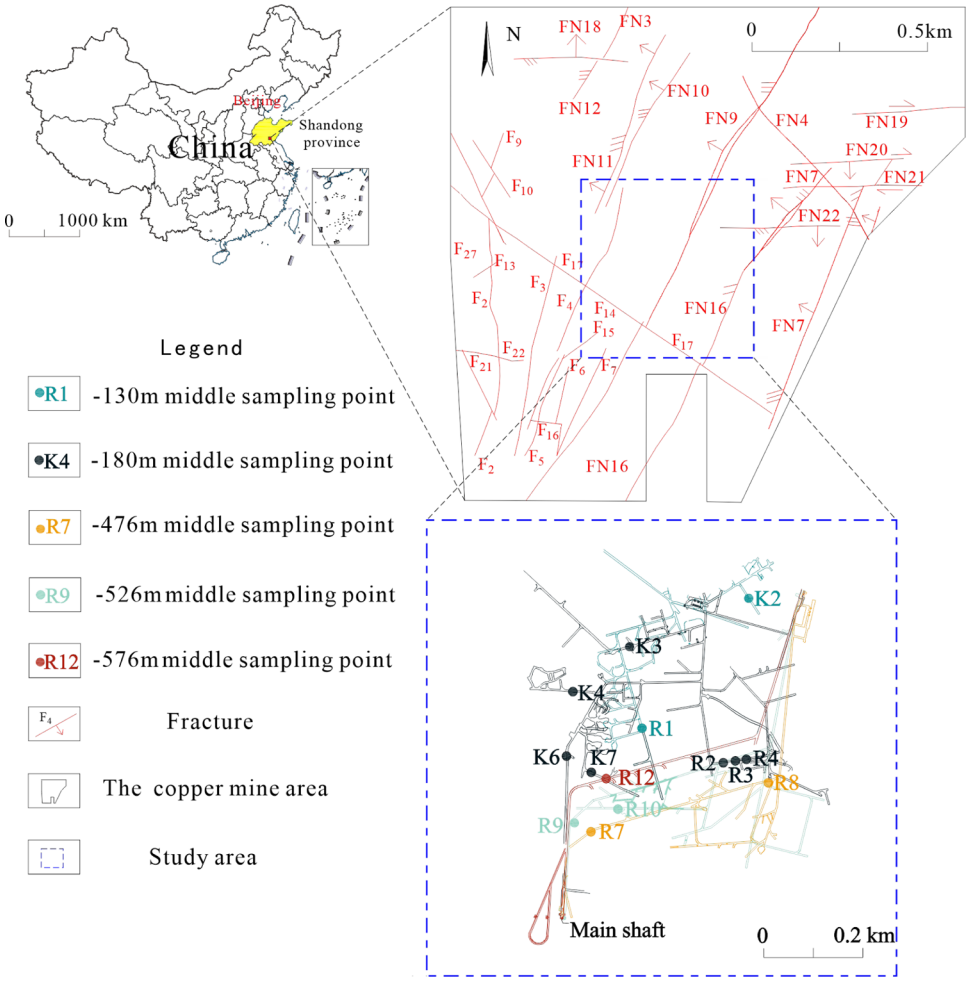

Figure 1. Mapping of the study area and sampling point.

temperature measurement, controllable source detection, and hydrochemical characteristic analysis to determine the geothermal anomalous area in the Wulian to Juxian section of the Yishu fault zone and calculated the geothermal reserves in the abnormal area. Jiang et al.[9] analyzed the source of geothermal water recharge, circulation conditions, and water−rock response through water chemistry and environmental isotope and concluded that the geothermal water in this region is mainly absorbed by the atmosphere. Precipitation replenishment and a large amount of cold water are mixed in during the mining process. Zhong et al.[10] determined that the geothermal system in Zhaoyuan City, Shandong province, belongs to a fracture-controlled geothermal reservoir by studying the geothermal genesis. The geothermal water recharge and upwelling channels are mainly the Zhaoping and Linglong faults, and the intersection is the geothermal water thermal cycle depth range. The geothermal water temperature in the Liuhangtou area, located on the Tangwu-Gegou Fault, can reach up to 60.96 °C. Geothermal heat comes from deep earth heat sources, magmatic-hydrothermal activity, and radioactive element metamorphosis, and the closer the temperature gradient is to the fracture zone, the higher the value.[11] The geothermal water in the Linyi section of the Yishu Fault Zone is mainly formed by atmospheric precipitation recharge, with a few deposits of ancient sedimentary water. The geothermal water conduction channel in the central part of Changle County on the western edge of the Yishushi Fracture Zone is the Tangwu-Gegou Fault and its sub-fractures, and the thermal storage is a deep circulation convective type of strip thermal storage.[12]

The current research on the geothermal water genesis model mainly focuses on the use of water chemistry and isotope analysis. However, the previous analysis of the geothermal water circulation depth takes relatively few factors into consideration, which will affect the accuracy of the geothermal water circulation depth. Therefore, to address this problem, the Si-enthalpy model and the isotope mass conservation method are combined to calculate the proportion of cold water mixing at each water sample point and use it as a weight to calculate the circulation depth, so that the results are more reasonable and in line with the actual situation. In this paper, mineral saturation indices, isotopic analysis ($\delta^{18}O$, δD), silica-enthalpy mixing equations, and geochemical geothermal temperature scales will be used to analyze the study area in terms of thermal reservoir temperature, recharge characteristics, mixing ratios, circulation depths, and fluid channels. After receiving recharge from the northwestern mountains and surrounding atmospheric precipitation, groundwater in the study area runs along the fracture zone in a south-easterly direction and receives heating from the surrounding rocks, with the water level at the fracture zone intersection. The water level at the fracture zone confluence rises, and the water is stored in the lower and middle Cambrian thermal reservoirs and continues to receive heating from deeper heat sources. The model of geothermal

https://doi.org/10.1021/acsomega.2c05936
ACS Omega 2022, 7, 43231−43241

Table 1. Statistical Description of Hydrochemical Parameters

	water temperature (°C)	Na^+(mg/L)	Ca^{2+}(mg/L)	Cl^-(mg/L)	SO_4^{2-}(mg/L)	TDS (mg/L)	δD (‰)	$\delta^{18}O$ (‰)
max	66.1	296	393	257	1904	3472	−65.96	−6.11
min	20.8	30.8	86.8	66.40	310	481	−80.61	−19.22
median	40.15	91.30	113.5	117.5	399.5	1155	−67.79	−9.83

water genesis in the copper well mining area of Yinan Gold Mine is thus established to reveal the genesis and circulation pattern of geothermal water.

2. GEOLOGICAL, HYDROGEOLOGICAL, AND CLIMATIC SETTINGS

The study area (Figure 1) is Yinan County, Linyi City, Shandong Province, China, with coordinates *X*: 3 940 719.65−3 943 174.57; *Y*: 39 633 496.60−39 634 466.64 and an area of 4.853 km^2. The mine is located in a warm-temperate semi-humid continental monsoon climate zone with an average annual temperature of 12.9 °C. The average annual precipitation in the mine area is 684.4 mm, with the maximum annual precipitation occurring between June and September when 73% of the annual rainfall occurs. The study area has a well-developed water system, with the River Yi to the east of the study area and the River Wen to the west flowing from north to south into the River Yi, which is a perennial flowing river; the River Tongjing flows from north to west to south to east through the area.

The stratum in the study area belongs to the Luxi stratigraphic division of the North China stratigraphic area. The stratigraphic basement is the Taishan Group of Archaeozoic, and the cover consists of the Upper Paleozoic Tumen Group, Paleozoic Cambrian, Ordovician, and Carboniferous, Jurassic of Mesozoic, Cretaceous, and Quaternary Cenozoic. The study area is located in the dislocated upwarping region of Central Shandong Province, with relatively well-developed fracture structures, dominated by the Tangwu-Gegou Fault in the NE-oriented Yishu Fault Zone, followed by NW and NE-oriented fractures intersecting the Yishu Fault Zone. Four of these fractures, F7, F5, F16, and F9, the larger extension and distribution scales, are highly correlated with the formation of the copper well geothermal field. The F7 fracture is the westernmost fracture in the Yishu Fracture Zone, with a local width of 30−40 m, which develops a large number of angular breccias such as limestone, shale, and sandstone, with intrusions of diorite porphyrite. F16 and F9 faults are roughly parallel to F7 and exposed on the ground, which plays a certain role in controlling the formation and distribution of copper well rock and copper well geothermal field. F5 is an NW-trending fracture, striking 315°, trending SW, dip 70°, and extending SE to lie beneath the Quaternary. Due to the long-term activity of the fault structure, the magmatic activity is multistage, which makes the intrusive rock types in the area complex, and the lithology and lithofacies change greatly. Magmatic rocks can be divided into copper well rock mass and Chaoyang rock mass according to different exposure sites. The copper mine rock body is a diorite complex, mainly composed of diorite porphyrite and diorite, and the secondary rock body is granodiorite. The diorite is mainly distributed in the western area of the copper well rock mass, and the diorite porphyrite is mainly distributed in the eastern part of the rock mass. The area from eastern Chaoyang to Da Chaoyang to the north of the mining area is the main concentration area of the Chaoyang pluton. Only the southern edge is exposed in the area, mainly composed of porphyritic amphibole syenite porphyrite and angular diorite porphyrite.

The aquifer is thin, has limited water storage capacity, is far from the ore body, and is not closely associated with the water-filling of the deposit. The Carbonate rock with clastic rock fissure karst aquifers are mainly located in the north and west of the copper mine and consist of limestone (marble), hornstone, and sandstone of Zhangxia Formation of Jiulong Group and Zhushadong Formation of Changqing Group. The metamorphic rock- and magmatic rock-weathered fissure water aquifers are mainly amphibolite quartz diorite porphyrite and quartz diorite porphyrite, distributed over a large area to the east and north of the mine area and have a weaker water abundance.

3. SAMPLING AND LABORATORY ANALYSIS

A total of 14 groundwater samples were collected in October 2021 from the north wind shaft to the main shaft in the eastern section of the copper well mine in the study area (Figure 1), and the temperature of the water samples was measured on-site using a portable thermometer. Geothermal water samples were stored in 500 mL high-density polyethylene bottles to ensure that the samples were filled to capacity and did not produce air bubbles during the sampling process. Water temperature and TDS were measured in the field using an SX713 TDS meter (0.1% precision) with a 2301-S plastic-housing conductivity electrode. Major element concentrations were completed at Shandong Huabiao Testing Co., Ltd. in Qingdao, Shandong Province. Na^+ and Ca^{2+} were measured using a Shimadzu AA-6000CF atomic absorption spectrophotometer with an anion charge balance error of <10%. Anions such as Cl^- and SO_4^{2-} were measured using an ICS-2100 ionophore chromatograph; $\delta^{18}O$ and δD were measured using an L2130-i isotope and gas concentration analyzer, and the precision of $\delta^{18}O$ and δD were 0.01 and 0.01‰, respectively. The specific water chemistry parameters at the sampling sites are shown in Table 1.

4. ORIGIN OF HOT WATER IN THE STUDY AREA

4.1. Estimation of Reservoir Temperature. As it is difficult to achieve an ideal mineral equilibrium state during the transport of hot water through underground channels,[13,14] the saturation indices of various minerals at different hot water temperatures were calculated and simulated using PHREEQC to differentiate the water−rock equilibrium state of the hot water (Figure 2)

$$SI = \log(IAP)/K_{sp} \quad (1)$$

where IAP is an ion activity product and K_{sp} is an equilibrium constant.

According to the results of the chemical equilibrium of geothermal water (Figure 2), the water samples in the deep region of the study area are more saturated than those in the shallow region, indicating that the water−rock interaction in the deep region is more intense than that in the shallow region.[15] However, since the saturation indexes of the above water samples except quartz and chalcedony have not reached

https://doi.org/10.1021/acsomega.2c05936
ACS Omega 2022, 7, 43231−43241

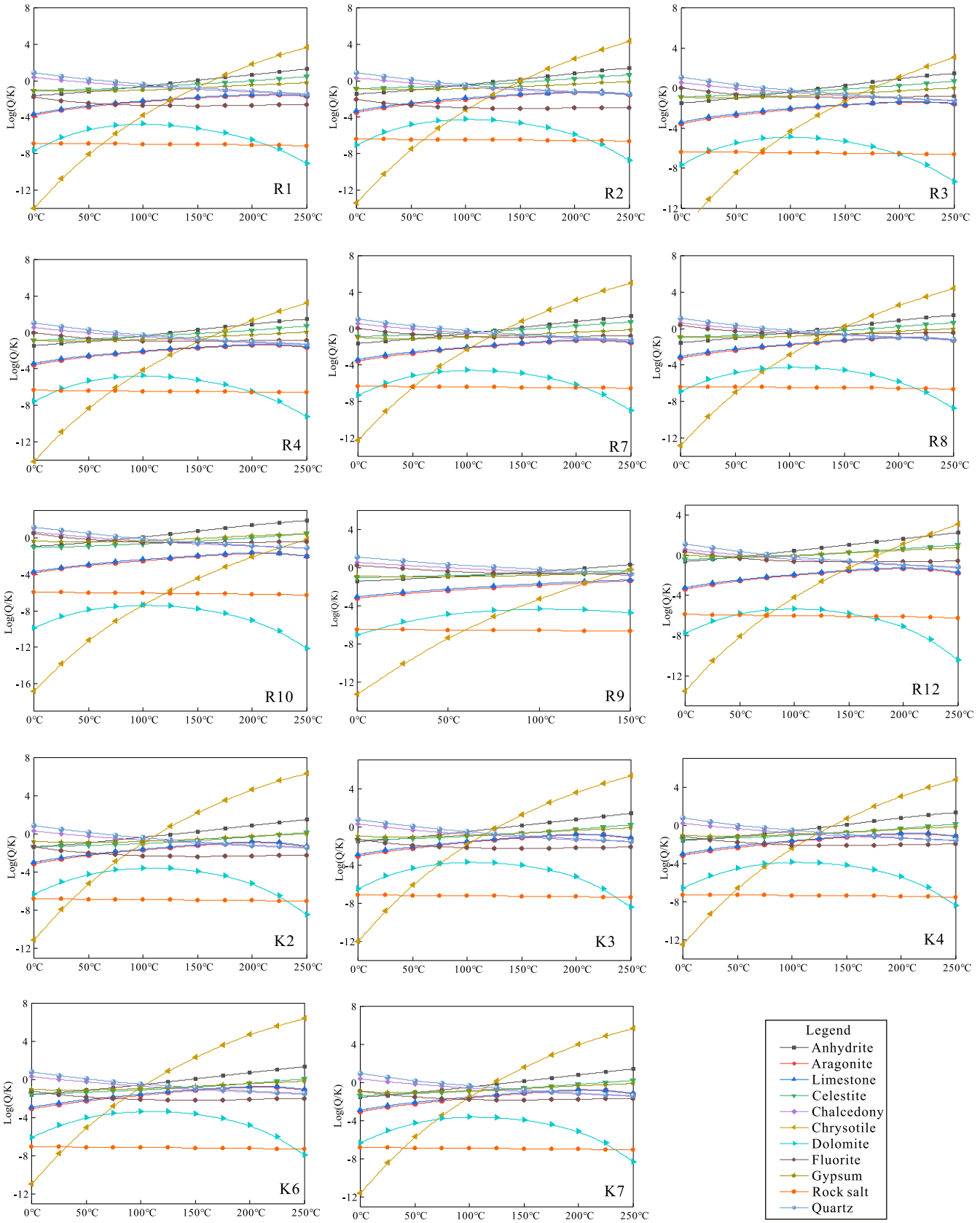

Figure 2. Simulation of multimineral saturation index of geothermal water in the study area.

saturation, the cation temperature scale cannot be selected to estimate the heat storage temperature.[16−18] Therefore, the SiO_2 temperature scale is selected for calculation:

Temperature scale 1: Quartz temperature standard without steam loss:

https://doi.org/10.1021/acsomega.2c05936
ACS Omega 2022, 7, 43231−43241

Table 2. Statistics of Geothermal Water Parameters in the Study Area

number	sampling site	temperature scale 1	temperature scale 2	temperature scale 3	temperature of the recharge area	method 1	method 2
R1	the −130 m level of the old well	61.22	66.98	29.07	7.54	1412.70	438.19
R2	the −180 m level of the old well	58.26	64.33	25.99	7.84	1382.33	216.39
R3	the −180 m middle section of the old well	78.23	82.02	46.82	7.83	1384.03	454.00
R4	the −180 m level of the old well	74.88	79.07	43.31	8.06	1360.42	333.35
R7	the −476 m level of Jinlong east district	77.69	81.54	46.25	8.07	1359.48	314.12
R8	the −476 m level of Jinlong east district	83.28	86.45	52.15	8.14	1352.95	21.50
R9	the −526 m level of Jinlong east district	81.28	84.69	50.03	8.17	1349.79	102.40
R10	the −526 m level of Jinlong east district	89.78	92.13	59.03	3.80	1786.99	310.71
R12	the −576 m level of Jinlong east district	82.39	85.67	51.20	7.47	1419.82	160.31
K2	the −130 m level of the old well	61.22	66.98	29.07	7.58	1408.76	142.80
K3	the −180 m level of the old well	52.05	58.79	19.60	8.54	1312.35	261.82
K4	the −180 m level of the old well	49.78	56.75	17.27	8.68	1298.73	1029.56
K6	the −180 m level of the old well	58.09	64.19	25.83	8.18	1348.69	304.15
K7	the −180 m level of the old well	66.79	71.93	34.85	8.45	1322.07	360.68

Table 3. Cold Water Mixing Ratio and Deep Hydrothermal Temperature of Each Sampling Point in the Study Area

	silicon−enthalpy equation method		silicon−enthalpy diagram method		isotope mass conservation method		mean	
number	temperature (°C)	mixing ratio (%)	temperature (°C)	mixing ratio (%)	K-terminal mixing ratio (%)	M-terminal mixing ratio (%)	temperature (°C)	mixing ratio (%)
R1	78.05	73.74	75.80	73.13	0.23	0.77	76.93	74.67
R2	64.36	48.83	60.26	47.84	0.17	0.83	62.31	60.00
R3	108.85	65.78	104.35	64.57	0.17	0.83	106.60	71.33
R4	100.64	66.02	100.21	65.87	0.13	0.87	100.43	73.00
R7	101.29	60.66	100.48	60.38	0.12	0.88	100.88	69.67
R8	115.69	63.41	106.71	60.04	0.11	0.89	111.20	70.67
R9	88.33	27.48	88.15	29.30	0.10	0.9	88.24	48.67
R10	111.85	46.56	106.71	44.51	1.00	0	109.28	30.67
R12	113.39	62.53	107.71	60.87	0.25	0.75	110.55	66.33
K2	74.88	71.08	74.73	71.05	0.23	0.77	74.80	73.00
K3	152.35	87.16			0.03	0.97	152.35	92.00
K4	180.49	95.33			0.00	1	180.49	97.50
K6	69.89	68.12	62.84	65.16	0.10	0.9	66.36	74.33
K7	108.14	84.15	103.91	83.63	0.05	0.95	106.03	87.67

$$T\ (^{\circ}\mathrm{C}) = \frac{1309}{5.19 - \lg \mathrm{SiO_2}} - 273.15 \quad (2)$$

Temperature scale 2: Quartz temperature standard with sufficient steam loss:

$$T\ (^{\circ}\mathrm{C}) = \frac{1522}{5.75 - \lg \mathrm{SiO_2}} - 273.15 \quad (3)$$

Temperature scale 3: Temperature standard of chalcedony without steam loss:

$$T\ (^{\circ}\mathrm{C}) = \frac{1032}{4.69 - \lg \mathrm{SiO_2}} - 273.15 \quad (4)$$

SiO_2 is the content of SiO_2 in geothermal water, and the unit is mg/L.

According to the calculation results (Table 2), compared with the actual temperature of the water sample, the error of the thermal storage temperature estimation results of the chalcedony thermometer is small, and the calculation results are between 17 and 60 °C, which is more consistent with the actual temperature, while the estimated values of the quartz thermometer without steam loss and the quartz thermometer with sufficient steam loss are between 49 and 90 °C and 56 and 92 °C, respectively. Because the SiO_2 temperature scale method ignores the influence of cold water mixing on geothermal water, the SiO_2 content decreases, and the result is low. Therefore, the calculated results of the SiO_2 geothermal temperature scale are taken as the reservoir temperature of the shallow region (−130 to −180 m), which is 53−81 °C. The average value of the calculated results of the SiO_2 geothermal temperature scale and silicon−enthalpy mixed model method is taken as the heat storage temperature of the deep region (−476 to −576 m), which is 85−97 °C.

4.2. Characteristics of the Contributing Region. The δD and δ^{18}O of atmospheric precipitation are proportional to the temperature. The temperature of the contributing region is calculated using the δD value and average temperature of atmospheric precipitation in China[19,20]

https://doi.org/10.1021/acsomega.2c05936
ACS Omega 2022, 7, 43231−43241

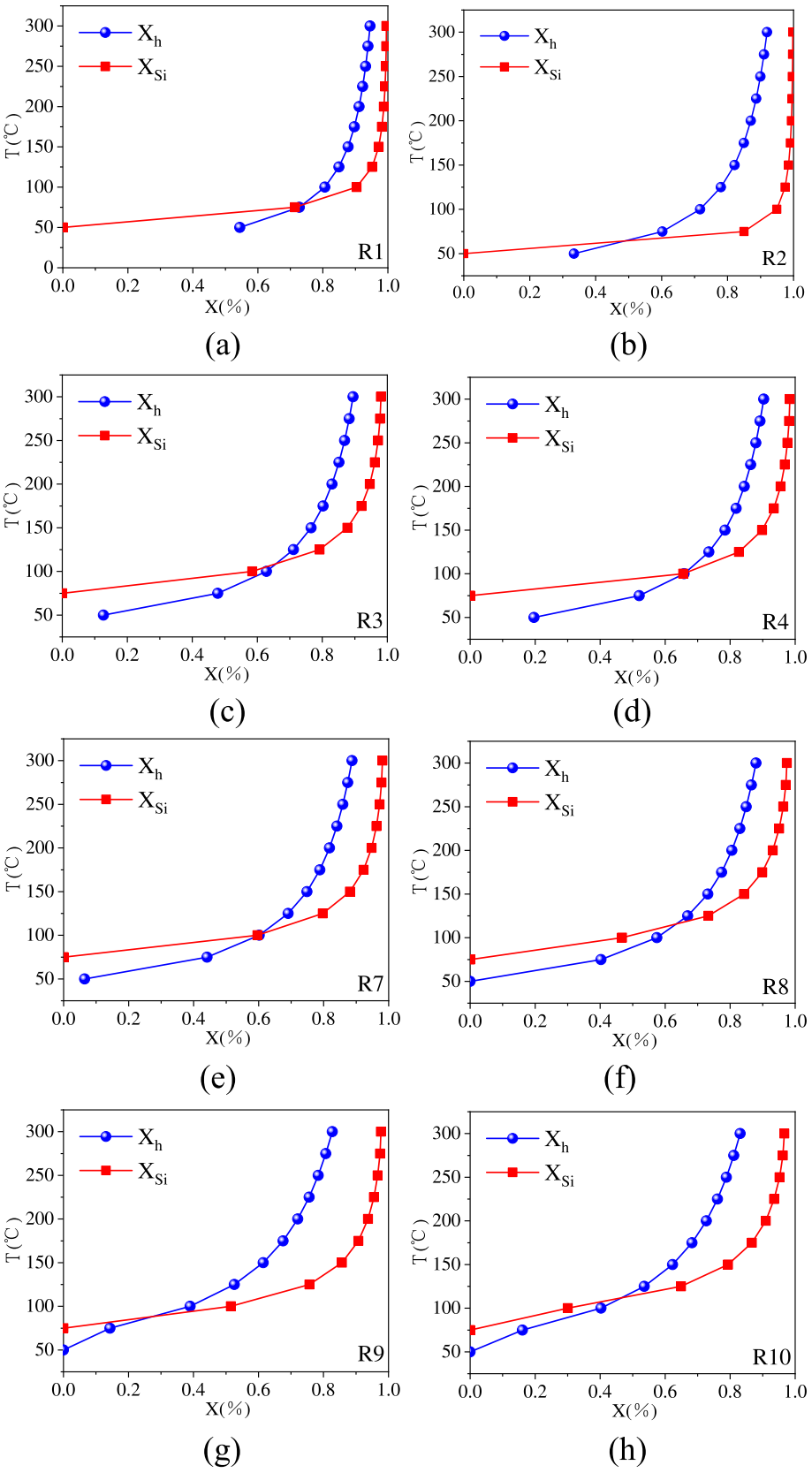

Figure 3. continued

https://doi.org/10.1021/acsomega.2c05936
ACS Omega 2022, 7, 43231−43241

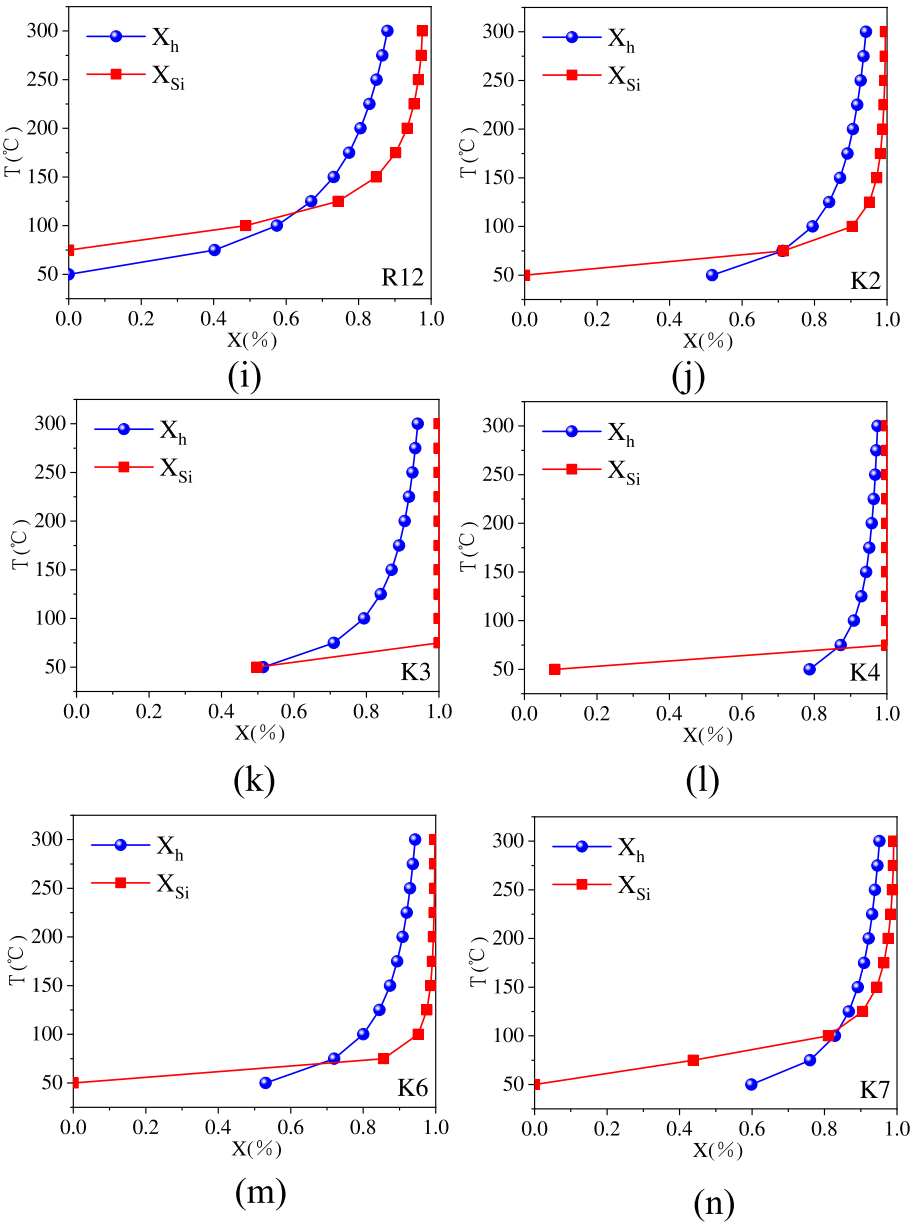

Figure 3. Relationship chart of mixing ratio of hot−cold water: (a) Mixing ratio relationship of R1. (b) Mixing ratio relationship of R2. (c) Mixing ratio relationship of R3. (d) Mixing ratio relationship of R4. (e) Mixing ratio relationship of R7. (f) Mixing ratio relationship of R8. (g) Mixing ratio relationship of R9. (h) Mixing ratio relationship of R10. (i) Mixing ratio relationship of R12. (j) Mixing ratio relationship of K2. (k) Mixing ratio relationship of K3. (l) Mixing ratio relationship of K4. (m) Mixing ratio relationship of K6. (n) Mixing ratio relationship of K7.

$$\delta D = 3t - 92 \quad (5)$$

It can be seen from Table 3 that the supply temperature in the study area is 7−9 °C, which is slightly lower than the annual average temperature of 12.9 °C. It is speculated that the reason is that the elevation value of the recharge area is large. The elevation of the contributing region is calculated mainly through the elevation effect of the δD value of atmospheric precipitation in China, or the recharge elevation of the relationship between the $\delta^{18}O$ value in groundwater and local altitude is calculated in two ways.[21−23] To reduce the estimation error of geothermal water recharge elevation in the study area, the average value of the two formulas is used as the recharge elevation value in the study area.

Method 1: Elevation effect of δD value of atmospheric precipitation in China:

$$\delta D = -0.03H - 27 \quad (6)$$

Method 2: Recharge elevation of the relationship between $\delta^{18}O$ value in groundwater and local altitude:

$$H = (\delta^{18}O_G - \delta^{18}O_S)/K + h \quad (7)$$

where H is the elevation of the geothermal water contributing region, m; h is the ground elevation of the geothermal water sampling point, m; $\delta^{18}O_G$ is the actual measurement of geothermal water sampling point $\delta^{18}O$ value (‰); $\delta^{18}O_S$ refers to the atmospheric precipitation near the sampling point $\delta^{18}O$ value (‰); and K is elevation gradient of atmospheric precipitation $\delta^{18}O$ value (−δ‰/100 m).

According to Table 2, the elevation of the geothermal water contributing region is 687.22−1164.15 m. Therefore, it is speculated that the water replenishment region is from the

https://doi.org/10.1021/acsomega.2c05936
ACS Omega 2022, 7, 43231−43241

mountain ranges with an altitude of more than 600 m distributed in the west and northwest of the study area, such as the Xinpu mountain uplift fault block, Huangshi mountain, Foshan top, and other mountain ranges and the surrounding atmospheric precipitation infiltration.

4.3. Cold and Hot Water Mixing Ratio. *4.3.1. Calculation of Hydrogen and Oxygen Isotopes.* The analysis shows that it is concluded that the local atmospheric precipitation and geothermal primary water (alpine snow melt water or high-altitude atmospheric precipitation) have a mixed recharge effect on the geothermal water in the study area; therefore, R10 and K4 are set as the input end elements K and M. The mixing ratio can be derived from the isotope mass conservation principle.[24]

$$\delta D_H = \delta D_K \cdot X + \delta D_M \cdot (1 - X) \quad (8)$$

where δD_H is mixed water δD value (‰); δD_K, δD_M is the value of input terminals K and M δD value (‰); and X is the mixing ratio of the input terminal K.

According to the calculation results in Table 3, it can be seen that the geothermal water in the study area, except for R10, is largely supplied by the M-end, that is, the local atmospheric precipitation. And with the continuous decrease of depth, the greater the influence of local atmospheric precipitation, and the higher the proportion of geothermal water in the region, the lower the mixing proportion of geothermal original water from high-altitude atmospheric precipitation or alpine ice and snow melt water, which indicates that the M-end is. The main recharge source of geothermal water in the study area is the local atmospheric precipitation with strong infiltration recharge. In addition, the environment of deep geothermal water is relatively closed, and the proportion of recharge from shallow cold water infiltration is small.

4.3.2. Estimation of the Silicon–Enthalpy Equation. To calculate the reservoir temperature of geothermal water and the mixing ratio of cold and hot water more accurately, a silicon–enthalpy mixing model is established for further analysis. The linear relationship between the enthalpy value and the SiO_2 content during the exchange and mixing of cold and hot water is expressed by the following formula[25−27]

$$H_c X_h + H_h(1 - X_h) = H_s \quad (9)$$

$$Si_c X_{Si} + Si_h(1 - X_{Si}) = Si_s \quad (10)$$

where H_c is the enthalpy of cold water in the shallow area of the study area, which is 12.9 × 4.1868 J/g; H_h is the original geothermal water enthalpy value in the deep part of the study area, and H_s is the enthalpy value of the water samples collected in the middle sections of the study area. All enthalpy values are the corresponding temperatures of the geothermal water. Si_c is the SiO_2 content in the geothermal water in the shallow part of the study area, which is 15.75 mg/L; Si_h is the SiO_2 content of deep geothermal water; Si_s is the SiO_2 content in hot water after mixing; and X is the proportion of hot water mixed with cold water in the shallow area.

It can be seen from Figure 3 that the silicon–enthalpy curves of each water sample have intersection points, among which the mixing ratio of K4 point is the highest, which is 95.33%, and the mixing ratio of R10 point is the lowest, which is 27.48%, and the mixing ratio of other middle water samples is between 46.56 and 87.16%. Overall, the vertical characteristics of the study area are significant, and the proportion of geothermal water mixed with cold water is relatively high, showing that the shallower the buried depth of geothermal water, the larger the proportion of cold water and the high-value areas are concentrated near the shallow fracture fault zone. It also shows that the fracture channel caused by the fault can easily be mixed with cold water for replenishment.

4.3.3. Silicon–Enthalpy Graphical Estimation. The silicon–enthalpy diagram method analyzes the thermal storage temperature and mixing ratio of hot and cold water in the research area before mixing.[28] The hypothetical condition of this method is that geothermal water does not exchange heat and mass loss with the surrounding rock and other materials when it moves along the water channel. The mixing of cold water only causes the temperature drop of the hot water, and no obvious chemical reaction and precipitation or dissolution of SiO_2 occurs during the mixing process. As shown in Figure 4, let point a be the SiO_2 content and enthalpy value of the cold water in the shallow part of the study area, and point B be the SiO_2 content and temperature of the water samples taken in the middle section. Connecting two points A and point B and making the extension line intersect the quartz solubility curve as point C, the abscissa corresponding to point C is the initial enthalpy of the deep geothermal raw water at the point, and the ratio of AB to AC line length is the proportion of hot water in the mixed water.

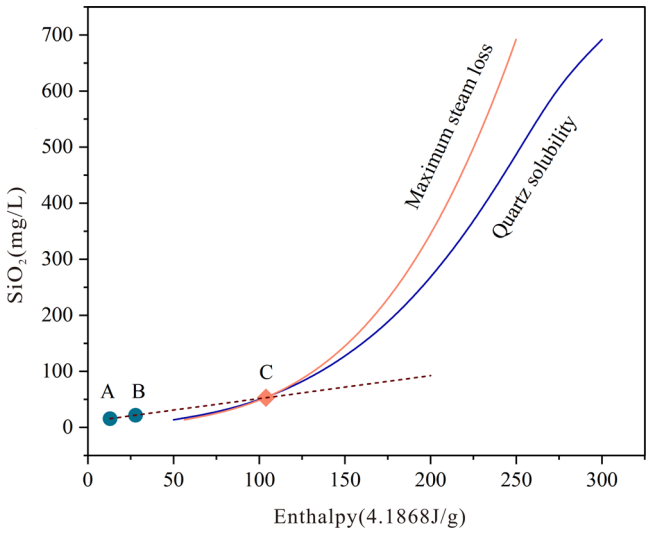

Figure 4. Silicon–enthalpy diagram method.

The results show that there are intersections between K3 and K4 water samples and the solubility curve of quartz, except that there are no intersections. To make the calculation results more reasonable and accurate, the average value of the silicon–enthalpy diagram method combined with the isotope mass conservation method and silicon–enthalpy equation method is used as the final solution of the mixing ratio of hot and cold water in geothermal water in the study area.

According to the calculation results (Table 3), the vertical distribution of hot water characteristics in the study area is more significant than in the plane. Through comparative analysis of the above methods, it is concluded that the proportion of cold water mixed at point K4 is the highest, reaching 97.5%, and the average proportion of cold water mixed at point R10 (−130 to −180 m) is 78.17%, the lowest proportion of cold water mixed at point R10 is 30.67%, and the average proportion of cold water mixed at a point deep (−476

https://doi.org/10.1021/acsomega.2c05936
ACS Omega 2022, 7, 43231−43241

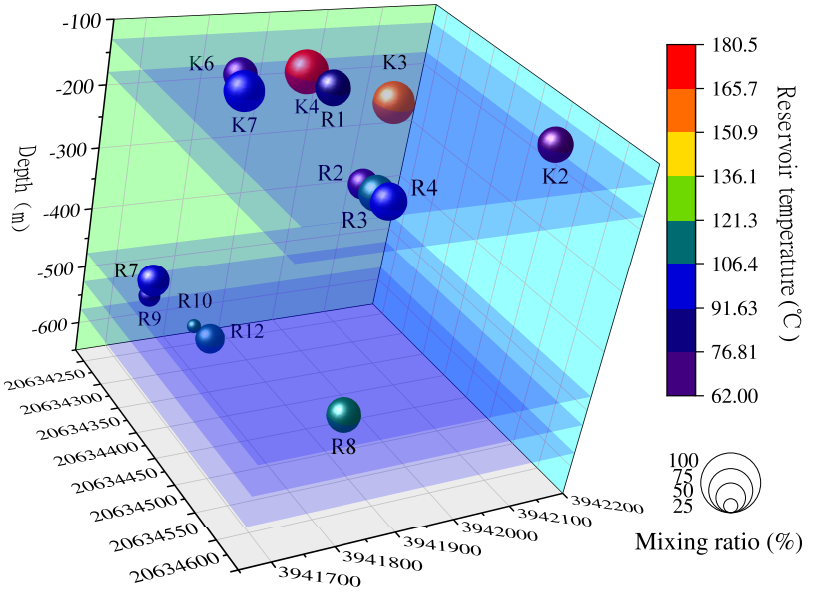

Figure 5. Distribution characteristics of silicon−enthalpy of water samples in each middle section of the study area.

Table 4. Depth of Geothermal Water Circulation in the Study Area

number	G(m/°C)	T_z (°C)	T_0 (°C)	Z_0 (m)	T_1 (°C)	Z_1 (m)	Z_2 (m)	Z (m)
R1	2.5	64.10	12.9	30	29.8	2078	1868	1921
R2	2.5	61.30	12.9	30	37.6	1966	2492	2282
R3	2.5	80.13	12.9	30	45.3	2719	3108	2996
R4	2.5	76.98	12.9	30	42.7	2593	2900	2817
R7	2.5	86.70	12.9	30	47.6	2982	3292	3198
R8	2.5	93.64	12.9	30	50	3260	3484	3418
R9	2.5	84.74	12.9	30	66.1	2903	4772	3813
R10	2.5	97.06	12.9	30	65	3397	4684	3791
R12	2.5	92.87	12.9	30	50	3229	3484	3398
K2	2.5	64.10	12.9	30	30.8	2078	1948	1983
K3	2.5	55.42	12.9	30	30.9	1731	1956	1938
K4	2.5	53.27	12.9	30	20.8	1645	1148	1160
K6	2.5	61.14	12.9	30	30.3	1960	1908	1921
K7	2.5	69.36	12.9	30	27.8	2288	1708	1780

to −576 m) is 57.2%. The overall geothermal water in the area is greatly affected by the mixing of cold water and is shown in Figure 5.

4.4. Circulation Depth. Considering that the groundwater in the study area is mixed with cold water to different degrees, the mean value X% of the overall geothermal water mixing ratio in the study area calculated by the silicon−enthalpy model and isotope mass conservation method is taken as the weight of the above formula to make the calculation result more reasonable. The calculation formula for geothermal water circulation depth in the study area is

$$Z = Z_1 \times (1 - X) + Z_2 \times X \tag{11}$$

$$Z_1 = 100 \times \frac{(T_Z - T_0)}{G} + Z_0 \tag{12}$$

$$Z_2 = 100 \times \frac{(2T_1 - T_0)}{G} \tag{13}$$

where Z is the geothermal water circulation depth; Z_1 is the circulation depth without cold water mixing (m); Z_2 is the circulation depth under the action of cold water mixing (m); Z_0 is the normal temperature layer thickness (m), taken as 30 m; G is the geothermal heating level (°C/100 M), taking 2.5 °C; T_0 is the annual average temperature in the study area (°C), taking 12.9 °C; T_Z is the heat storage temperature (°C); and T_1 is the temperature (°C) of geothermal water in each middle section of the study area.

According to the calculation results of circulation depth (Table 4), the hot water circulation depth of the K4 water sample point is the smallest, 1160 m, and the hot water circulation depth of the R9 water sample point is the largest, 3813 m, and the temperature is 65 °C. The actual measured temperatures of K4 and R12 water sample points are 20.8 and 66.1 °C, respectively, which is in line with the actual situation. On the whole, the temperature of the shallow geothermal water in the study area is lower, and the circulation depth of the geothermal water is smaller, ranging from 1160 to 2996 m, and the average depth is 2089 m. The temperature of deep geothermal water is high, and the circulation depth of hot water is large, 3198−3813 m, with an average depth of 3524 m.

https://doi.org/10.1021/acsomega.2c05936
ACS Omega 2022, 7, 43231−43241

5. DISCUSSION

Geothermal resources are environmentally friendly and sustainable, and their use has improved the current energy structure and ecological quality in China and the world. China is rich in geothermal resources, and if they are fully utilized, it is of great significance for the development of China. The key to the full utilization of geothermal resources lies not only in the study of the research area but also in the study of the geothermal genesis mechanism of the entire structure to realize the large-scale exploitation of geothermal resources in the whole region as a whole.

Combined with the analysis in this paper, the infiltration of atmospheric precipitation in the northwestern mountain range of the study area recharges groundwater, which is transported through fracture zones and receives heating from the surrounding rocks. The water level is raised at the intersection of the fracture zones and stored in the middle and lower Cambrian thermal reservoirs. It continues to receive heating from deeper heat sources. Based on calculations of recharge elevations, which range from 687.22 to 1164.15 m, it is assumed that the source of recharge is located in the northwestern mountains and surrounding atmospheric precipitation. The Yishu Fault Zone is the Shandong section of the Tanlu Fault Zone, which has a long and complex history of activity, originating early from the collisional orogeny of the North China and South China plates, where significant left-slip shear deformation occurred, forming a broad fracture zone and inducing volcanic eruptions and fault deposition. During the Mesozoic, a small amount of amphibolite intruded along the fractures, forming a large area of the Qingshan Group andesite cover, forming a good cover for the thermal reservoir, and the Cenozoic showed strong extrusion, forming a series of compressional structures. The deep-cut upper mantle fracture zone not only provides a channel for the deep circulation of groundwater but also accelerates the mixing of hot and cold water. Its heat source is not only the mantle heat flow but also the heat generated by the decay of radioactive elements and the activity of the fracture zone. The Yishu Fracture Zone has four main fractures; the nearest main fracture to the study area is the Tangyu-Gegou Fracture, and to the east of the Tangyu-Gegou Fracture is the Su-cun Depression, which provides good conditions for the recharge, transport, and continuous heating of geothermal water. It is assumed that the source of geothermal water not only comes from the northwestern mountains and the surrounding atmospheric precipitation recharge but also possibly from the Yishu Fracture Zone.

6. CONCLUSIONS

(1) The elevation of the recharge zone of geothermal water in the study area ranges from 687.22 to 1164.15 m, and the temperature of the recharge zone ranges from 7 to 9 °C. It is presumed that the mountains 600 m above sea level and the surrounding mountains in the western and northwestern parts of the study area are the recharge zones of geothermal water.

(2) The thermal storage of geothermal water in the study area is in the form of a belt with both layers, and the temperature of the deep geothermal water storage is 85−97 °C, and the circulation depth is 3198−3813 m, with an average depth of 3524 m. The temperature of the shallow geothermal water storage is 53−81 °C, and the circulation depth is 1160−2996 m, with an average depth of 2089 m. The thermal storage of shallow and deep geothermal water belongs to the category of low and medium-temperature thermal storage, and the geothermal water in the thermal storage has not reached the water rock balance.

(3) The groundwater in the eastern section of the copper well mining area of Yinan Gold Mine mainly receives infiltration recharge from atmospheric precipitation; the deep heat source heats the groundwater through the fracture zone conduction heat; the water level rises at the intersection of the F5 and F16 fractures, mixing with the shallow hot water; some of the geothermal water is recharged to the upper aquifer or excluded from the surface; and the remaining geothermal water is stored in the middle and lower Cambrian thermal reservoirs to form a geothermal anomaly or continues to run off along the fractures to recharge the fractured karst groundwater.

AUTHOR INFORMATION

Corresponding Author

Xinlong Zhou − *Dongli Town People's Government of Yiyuan County, Zibo 256119 Shandong, China;* orcid.org/0000-0003-0967-4303; Email: 13206449819@163.com

Authors

Huiyong Yin − *College of Earth Science and Engineering, Shandong University of Science and Technology, Qingdao 266590, China;* orcid.org/0000-0002-2752-765X

Chengwei Zhang − *College of Earth Science and Engineering, Shandong University of Science and Technology, Qingdao 266590, China*

Tao Chen − *College of Earth Science and Engineering, Shandong University of Science and Technology, Qingdao 266590, China*

Fangying Dong − *College of Earth Science and Engineering, Shandong University of Science and Technology, Qingdao 266590, China*

Wenju Cheng − *College of Earth Science and Engineering, Shandong University of Science and Technology, Qingdao 266590, China*

Ruqian Tang − *College of Earth Science and Engineering, Shandong University of Science and Technology, Qingdao 266590, China*

Guoliang Xu − *College of Earth Science and Engineering, Shandong University of Science and Technology, Qingdao 266590, China*

Peng Jiao − *Shandong Gold Mining (Yinan) Co., Ltd., Linyi 276300, China*

Complete contact information is available at: https://pubs.acs.org/10.1021/acsomega.2c05936

Author Contributions

X.Z. and P.J. collected the resources; P.J. conducted the investigation; H.Y. and C.Z. performed writing—original draft; X.Z. and W.C. performed supervision; H.Y. took care of funding acquisition; C.Z. and G.X. took care of methodology; T.C., F.D., and R.T. performed format analysis. All authors have read and agreed to the published version of the manuscript.

https://doi.org/10.1021/acsomega.2c05936
ACS Omega 2022, 7, 43231−43241

Funding

This research was funded by the National Natural Science Foundation of Shandong Province (Grant Number ZR2019MD013).

Notes

The authors declare no competing financial interest.

REFERENCES

(1) Zhao, X. G.; Guan, W. Current situation and prospect of Chinas geothermal resources. *Renewable Sustainable Energy Rev.* **2014**, *32*, 651−661.

(2) Cheng, Y.; Zhang, Y. Hydraulic Fracturing Experiment Investigation for the Application of Geothermal Energy Extraction. *ACS Omega* **2020**, *5*, 8667−8686.

(3) Pang, Z. H.; Luo, J.; Cheng, Y. Z.; Duan, Z. F.; Tian, J.; Kong, Y. L.; Li, Y. M.; Hu, S. B.; Wang, J. Y. Evaluation of geological conditions for deep geothermal energy exploitation in China. *Earth Sci. Front.* **2020**, *27*, 134−151.

(4) Bonte, M.; Roeling, W. F. M.; Zaura, E.; van der Widen Paul, W. J. J.; Stuyfzand, P. J.; Breukelen, B. Impacts of Shallow Geothermal Energy Production on Redox Processes and Microbial Communities. *Environ. Sci. Technol.* **2013**, *47*, 14476−14484.

(5) White, D. E.*Hydrology, Activity, and Heat Flow of the Steamboat Springs Thermal System, Washoe County, Nevada*; Center for Integrated Data Analytics, Wisconsin Science Center, 1968.

(6) Chiocchini, U.; Castaldi, F.; Barbieri, M.; Eulilli, V. stratigraphic and geophysical approach to studying the deep circulating groundwater and thermal springs, and their recharge areas, in Cimini Mountains - Viterbo area, central Italy. *Hydrogeol. J.* **2010**, *18*, 1319−1341.

(7) Battistel, M.; Hurwitz, S.; Evans, C. W.; Barbieri, M. The chemistry and isotopic composition of waters in the low-enthalpy geothermal system of Cimino-Vico Volcanic District, Italy. *J. Volcanol. Geotherm. Res.* **2016**, *328*, 222−229.

(8) Yang, B. G.; Zhu, W. Analysis and Research on thermal storage model of geothermal anomaly area in Wulian Juxian section of Yishu Fault Zone. *Acta Ecol. Sin.* **2019**, *93*, 192−196.

(9) Jiang, H. Y.; Wang, S. X.; Liu, L.; Cao, Y. L.; Shi, M.; Li, T. T.; Sun, W. G. Hydrochemical and environmental isotope characteristics of geothermal resources in Linyi section of Yishu Fault Zone. *J. Shanghai Land Resour.* **2018**, *39*, 90−94.

(10) Zhong, Z. N.; Kang, F. X.; Song, M. Z.; Lang, X. J.; Liu, L. Y.; Fu, P. Y.; Li, Z. J. Study on geothermal flux and geothermal genesis of Zhaoyuan geothermal field in eastern Shandong Province. *J. Geol. Rev.* **2021**, *67*, 828−840.

(11) Su, B. J.; Zhang, C.; Wang, W.; Liu, L.; Liu, A. T. Characteristics of geothermal resources in Liuhangtou area of Linyi City. *J. Shandong Land Resour.* **2015**, *31*, 31−35.

(12) Wang, Q.Investigation and Analysis of Geothermal and Thermogenic Geological Conditions in the Western Margin of Yishu Fault Zone and the Central Area of Changle County, Dissertation, Ocean University of China, 2013, pp 43−46.

(13) Zhou, X.; Ma, Z. Y.; Xi, L. P.; Dou, H. P. Study and Simulation of mixing action of thermal storage fluid in Xianyang City. *Ground Water* **2012**, *34*, 36−39.

(14) Xing, L. N.; Zhan, Y. H.; Guo, H. M. Groundwater hydrochemical characteristics and processes along flow paths in the North China Plain. *J. Asian Earth Sci.* **2013**, *70*−*71*, 250−264.

(15) Tu, C. L.; Yang, R. B.; Ma, Y. Q.; Linghu, C. W.; Zhao, R. G.; He, C. Z. Hydrochemical Evolution Characteristics and Driving Factors of Tuo Changjiang River Basin in West Guizhou. *J. Environ. Sci.* **2022**, 1−13.

(16) Zhuang, S. D.; Zhou, X. C.; Li, P. F.; Shi, Z. M.; Saimaiernaji, K.; Zhu, C. Y.; Yan, Y. C. Geochemical characteristics of hot spring environment in Tashkurgan fault zone, Xinjiang. *J. Earth Sci. Environ.* **2022**, *44*, 699−712.

(17) Wei, Z.; Shao, H.; Ling, T. D.; Bing, E.; Li, F.; Wang, B. Hydrogeochemistry and geothermometry of geothermal waters from the Pearl River Delta region, South China. *Geothermics* **2021**, *96*, No. 102164.

(18) Lu, Z. Q.; Song, H. J.; Cheng, H. Z. Estimating Radon Hot Spring Thermal Storage Temperature in Dasunzhuang, Pingyin County, Jinan City by Geothermal Temperature Standard. *Geol. Chem. Miner.* **2020**, *42*, 42−46.

(19) Zhou, S. J.; Sun, C. J.; Chen, W.; Zhang, X. Analysis of stable isotope characteristics and water vapor sources of precipitation in the eastern part of the Loess Plateau during the summer half year. *Acta Geogr. Sin.* **2022**, *77*, 1745−1761.

(20) Ye, X. Q.; Wu, G. D.; Yang, Y.; Huang, X. Hydrogen and Oxygen Stable Isotope Characteristics of Geothermal Spring Water in Shigaze Area, Tibet. *J. Environ Chem.* **2022**, 1−16.

(21) Liu, K.; Liu, Y. C.; Sun, Y.; Liu, J. R.; Wang, S. F.; Liu, Z. M. Analysis on Characteristics of Geothermal Water Deuterium Excess Parameters in Beijing. *Geol. China* **2015**, *42*, 2029−2035.

(22) Wang, J. Q.; Zhou, X.; Li, X. L.; Wang, M. M.; Shen, Y.; Fang, B. Chemical Characteristics and Origin Analysis of Hot Spring Water for Sheep Honey-eating in Lanping Basin, Yunnan Province. *Geoscience* **2017**, *31*, 822−831.

(23) Qu, X. Y.; Shi, L. Q.; Qu, X. W.; Qiu, M.; Gao, W. F.; Wang, J. Evaluation of Groundwater Resources and Exploitation Potential: A Case from Weifang City of Shandong Province in China. *ACS Omega* **2021**, *6*, 10592−10606.

(24) Lang, X. J.; Lin, W. J.; Liu, Z. M.; Xing, L. X.; Wang, G. L. Hydrogeochemical characteristics of underground hot water in Guide Basin. *Earth Sci.* **2016**, *41*, 1723−1734.

(25) Song, X. Q.; Peng, Q.; Duan, Q. S.; Xia, Y. L. Chemical Characteristics and Origin of Geothermal Water in Northeast Guizhou. *Earth Sci.* **2019**, *44*, 2874−2886.

(26) Yang, F. T.; Shi, Y. J.; Li, W. Q. Research on Formation Model of Geothermal Water in Dandong Area of Liaoning Province Based on Hydrogeochemical Characteristics. *Geoscience* **2022**, *36*, 474−483.

(27) Gupta, H.; Roy, S.*Geothermal Energy: An Alternative Resource for the 21st Century*; Elsevier, 2007; pp 73−74.

(28) Wang, X. C.Hydrochemical Characteristics and Hydrogeochemical Simulation of Hot Springs along the Lijiang River in Yunnan Province, Dissertation, China University of Geosciences: Beijing, 2016, pp 55−56.

https://doi.org/10.1021/acsomega.2c05936
ACS Omega 2022, 7, 43231−43241